

# Loss of Nicastrin from Oligodendrocytes Results in Hypomyelination and Schizophrenia with Compulsive Behavior<sup>\*[S]</sup>

Received for publication, January 11, 2016, and in revised form, March 23, 2016. Published, JBC Papers in Press, March 23, 2016, DOI 10.1074/jbc.M116.715078

Daniel R. Dries<sup>‡§</sup>, Yi Zhu<sup>‡</sup>, Mieu M. Brooks<sup>‡</sup>, Diego A. Forero<sup>¶</sup>, Megumi Adachi<sup>||</sup>, Basar Cenik<sup>‡</sup>, James M. West<sup>‡</sup>, Yu-Hong Han<sup>‡</sup>, Cong Yu<sup>‡</sup>, Jennifer Arbella<sup>§</sup>, Annelie Nordin<sup>\*\*</sup>, Rolf Adolfsen<sup>\*\*</sup>, Jurgen Del-Favero<sup>‡‡</sup>, Q. Richard Lu<sup>§§¶¶1</sup>, Patrick Callaerts<sup>|||</sup>, Shari G. Birnbaum<sup>||</sup>, and Gang Yu<sup>‡2</sup>

From the Departments of <sup>‡</sup>Neuroscience, <sup>||</sup>Psychiatry, and <sup>¶¶</sup>Developmental Biology, University of Texas Southwestern Medical Center at Dallas, Dallas, Texas 75390, the <sup>§</sup>Chemistry Department, Juniata College, Huntingdon, Pennsylvania 16652, the <sup>¶</sup>Laboratory of NeuroPsychiatric Genetics, Biomedical Sciences Research Group, School of Medicine, Universidad Antonio Nariño, 37-94 Bogotá, Colombia, the <sup>\*\*</sup>Division of Psychiatry, Department of Clinical Sciences, Umea University, SE-901 87 Umea, Sweden, the <sup>‡‡</sup>Applied Molecular Genomics Unit, VIB Department of Molecular Genetics, University of Antwerp, 2610 Antwerp, Belgium, the <sup>§§</sup>Department of Pediatrics, Cincinnati Children's Hospital Medical Center, Cincinnati, Ohio 45229, and the <sup>|||</sup>Laboratory of Behavioral and Developmental Genetics, Katholieke Universiteit Leuven Center for Human Genetics, VIB Center for the Biology of Disease, 3000 Leuven, Belgium

The biological underpinnings and the pathological lesions of psychiatric disorders are centuries-old questions that have yet to be understood. Recent studies suggest that schizophrenia and related disorders likely have their origins in perturbed neurodevelopment and can result from a large number of common genetic variants or multiple, individually rare genetic alterations. It is thus conceivable that key neurodevelopmental pathways underline the various genetic changes and the still unknown pathological lesions in schizophrenia. Here, we report that mice defective of the nicastrin subunit of  $\gamma$ -secretase in oligodendrocytes have hypomyelination in the central nervous system. These mice have altered dopamine signaling and display profound abnormal phenotypes reminiscent of schizophrenia. In addition, we identify an association of the *nicastrin* gene with a human schizophrenia cohort. These observations implicate  $\gamma$ -secretase and its mediated neurodevelopmental pathways in schizophrenia and provide support for the “myelination hypothesis” of the disease. Moreover, by showing that schizophrenia and obsessive-compulsive symptoms could be modeled in animals wherein a single genetic factor is altered, our work provides a biological basis that schizophrenia with obsessive-compulsive disorder is a distinct subtype of schizophrenia.

Psychiatric diseases such as schizophrenia, obsessive-compulsive disorder, attention deficit hyperactivity disorder, and autism exert devastating impact on the well-being of those affected and the society at large. The clinical symptoms and etiologies of these diseases are complex, obscure, and often overlap, and characteristics of these diseases can only be partially and incompletely captured in existing animal models. In contrast to classical neurological disorders such as Alzheimer disease, psychiatric disorders do not display overt neuropathological lesions but rather are attributed to changes in synaptic transmission, neuronal homeostasis, and neuronal networks. Both genetic and environmental factors contribute to these changes, which can result from multiple, individually rare genetic alterations or from large numbers of common genetic variants. Often, psychiatric disorders have their origins in perturbed neurodevelopment. It is therefore conceivable that key neurodevelopmental factors and pathways contribute to their neurobiological underpinnings.

Several important neurodevelopmental pathways are controlled by  $\gamma$ -secretase, a multisubunit, multitransmembrane-spanning proteolytic complex that cleaves a host of type I transmembrane proteins within the lipid bilayer (1). Although  $\gamma$ -secretase is perhaps best known for its role in cleaving the amyloid precursor protein in Alzheimer disease, key  $\gamma$ -secretase substrates have also been implicated in schizophrenia, most notably neuregulin-1 (Nrg1) and its receptor ErbB4 (2, 3). A recent study also demonstrated a functional interaction between the amyloid precursor protein and disrupted-in-schizophrenia-1 in cortical development (4). Moreover, multiple  $\gamma$ -secretase substrates have been directly or indirectly implicated in regulating myelination (5–8). In humans, white matter abnormality has long been suggested as a pathological lesion or a biomarker of schizophrenia, and a decrease in a host of myelin-related genes have been identified in chronic schizophrenia (2). Recent studies also point to defective myelination and the resulting changes in neural circuitry as an underlying cause of the disorder (9). It is in this context that we sought to

\* This work was supported by National Institute of Neurological Disorders and Stroke Grant R01 NS079796, by the National Institute on Aging Grant F32 AG031625, by the Hartwell Foundation, by the Fund for Scientific Research Flanders, by the Industrial Research Fund, by the Special Research Fund of the University of Antwerp, Belgium, by Swedish Medical Research Council Grant K2001–21X-10412-09A, and the County Council of Västerbotten and Norrbotten, Sweden. The authors declare that they have no conflicts of interest with the contents of this article. The content is solely the responsibility of the authors and does not necessarily represent the official views of the National Institutes of Health.

[S] This article contains supplemental Video S1.

<sup>1</sup> Present address: Dept. of Pediatrics, Cincinnati Children's Hospital Medical Center, Cincinnati, OH 45229.

<sup>2</sup> To whom correspondence should be addressed: Dept. of Neuroscience, University of Texas Southwestern Medical Center, 6000 Harry Hines Blvd., Dallas, TX 75390. Tel.: 214-648-5157; Fax: 214-648-1801; E-mail: gang.yu@utsouthwestern.edu.

## Schizophrenia- and OCD-like Behaviors in Nicastrin cKO Mice

examine the roles of oligodendrocyte  $\gamma$ -secretase in myelination and in psychiatric behaviors.

Here, we describe a conditional knock-out (cKO)<sup>3</sup> mouse in which nicastrin, the substrate receptor of  $\gamma$ -secretase, was deleted from oligodendrocytes, the myelinating cells of the central nervous system. We present evidence for the role of  $\gamma$ -secretase in schizophrenia-like behaviors, including the identification of putative SNPs in the nicastrin locus in a human schizophrenia/bipolar disorder cohort. The model described herein provides a powerful new tool for the dissection of several endophenotypes that belie multiple psychiatric disorders. Indeed, the cKO mouse presented here may help to reconcile the longstanding observation of comorbidity between schizophrenia and obsessive-compulsive behavior, indicating that this may indeed be a distinct—but substantial—subclass of schizophrenia.

### Experimental Procedures

**Reagents**—TRIZOL was purchased from Invitrogen; High Capacity cDNA Reverse Transcription Kit and SYBR green was from Applied Biosystems. All other reagents were reagent grade.

**Mice**—Floxed *nicastroin* and *olig1-cre* mice have been described elsewhere (10, 11). The mice were kept on a 12-h light/12-h dark cycle and given access to food and water *ad libitum*. To minimize variability in behavior caused by genomic heterogeneity, conditional knock-out mice were tested against littermate controls. *Olig1-cre* mice (*olig1*<sup>+/*Cre*</sup>) were first crossed with floxed *nicastroin* mice (*nicastroin*<sup>flox/flox</sup>) to generate single heterozygote (*olig1*<sup>+/*+*</sup>; *nicastroin*<sup>+/*flox*</sup>) and double heterozygote (*olig1*<sup>+/*Cre*</sup>; *nicastroin*<sup>+/*flox*</sup>) mice, nonsibling pairs of which in turn were crossed to one another to generate all three genotypes (*olig1*<sup>+/*Cre*</sup>; *nicastroin*<sup>+/*+*</sup>, *olig1*<sup>+/*+*</sup>; *nicastroin*<sup>flox/flox</sup>, and *olig1*<sup>+/*Cre*</sup>; *nicastroin*<sup>flox/flox</sup>) as littermates. The mice were genotyped by standard PCR of ear tissue (for genotyping details, see Ref. 10 and 11). All behavioral testing was conducted on sex-matched mice between 18 and 24 weeks of age unless stated otherwise. Experimentalists were blinded to genotype. All animal procedures conform to the Guide for the Care and Use of Laboratory Animals and were approved by the Institutional Animal Care and Use Committee at University of Texas Southwestern Medical Center.

**Quantitative Real Time PCR (qRT-PCR)**—RNA was extracted from either a pool of six pairs of optic nerves or cells purified by immunopanning using TRIZOL (Invitrogen). cDNA was synthesized using a high capacity cDNA reverse transcription kit (Applied Biosystems). qRT-PCR was performed using the ABI 7500 fast real time PCR system, with an initial denaturation for 20 min at 95 °C, followed by 40 cycles of 3 s of denaturation at 95 °C, and 30 s of annealing at 60 °C. Amplification of target genes was measured using the fluorescent dye SYBR green (Applied Biosystems), and data were collected during each annealing phase. Each qRT-PCR run was performed in triplicate, with data representing three experimental replicates

(i.e. three separate sets of six optic nerve pairs). Fluorescence intensity was plotted against cycle number for each sample to extract  $C_t$  values, which in turn were standardized to the house-keeping gene *u36b*. The data are presented as fold change of mRNA relative to transcript levels in the Cre mice. The primers used are as follows: *u36b*, forward 5'-cgtcctcgttgagtgac-3', reverse 5'-cgggtcgcgcagggattg-3'; *cyclophilin*, forward 5'-ggagatggcacaggaggaa-3', reverse 5'-gccctagtgcttcagctt-3'; *actinB*, forward 5'-gggggatatgggtcagaaggac-3', reverse 5'-ggctggggtgtgaaggtctc-3'; and *nicastroin*, forward 5'-gggcaagctcttcaccagagatgta-3', reverse 5'-ggcaagaccagcgatttacttctggt-3'.

**Electron Microscopy**—Details for the collection, staining, and analysis of tissues are provided elsewhere (11). Measurements for the quantification of *g* ratios were taken from electron micrographs of three 6-month-old animals per genotype and at least 100 myelinated axons per micrograph. The degree of myelination can vary by axonal diameter, with smaller axons typically having lower *g* ratios (see Fig. 1). Therefore, to eliminate any confounder of the distribution of axonal diameters within a sample, axons were binned by 0.1  $\mu$ m, and randomized block design using repeated measures two-way (genotype and axonal diameter bin) ANOVA was used to calculate the mean *g* ratio  $\pm$  S.E. across the three examined genotypes. Cumulative frequency plots with respect to *g* ratio were also constructed.

**Behavioral Tests**—For the force plate actimeter/open field, mice were habituated to the test room for 1 h prior to testing. Mice were then placed into the center of a 44  $\times$  44-cm platform of a force plate actimeter (BASi). The mice were allowed to explore the platform for 30 min, and data were collected at 100 points per second and 1024 s per frame. The first 10 min of activity was considered as a period of habituation to the apparatus and was therefore discarded from analysis. The displayed tracings are representative of the median four mice of each genotype from a pool of at least 18 mice and comprise 5 min of activity 15 min into the experiment. Details for the elevated plus maze are found in Ref. 12; those for prepulse inhibition and grooming are provided in Ref. 13.

**Haloperidol Treatment**—Haloperidol (Sigma) powder was dissolved in glacial acetic acid to form a 50 mg/ml concentrated stock. The stock solution was dissolved 1000-fold in 0.9% bacteriostatic saline and brought to pH 6.5 by the dropwise addition of 1 N NaOH, vortexing vigorously. Vehicle was prepared likewise. The mice were injected intraperitoneally at a dose of 0.25 mg/kg haloperidol (ED<sub>50</sub> of haloperidol = 0.2 mg/kg (14). Higher doses of haloperidol rendered the mice catatonic.

**Statistical Analysis of Behavioral Data**—All data are presented as means  $\pm$  S.E. Behavioral data were first analyzed by sex, with a minimum of four mice per sex. Student's *t* tests revealed no statistically significant difference in the performance of male and female mice on any of the measured behavioral tests. Data from both sexes were pooled for a given genotype with a minimum of eight mice per genotype. After pooling of data, single outliers were removed within an experiment only if justified by using the Grubbs' outlier test. One-way ANOVA with a Bonferroni post hoc test was used for tests containing the three genotypes and one parameter (e.g. open field locomotion). Two-way ANOVA with a Bonferroni post hoc test was used for tests containing the three genotypes and two parameters (e.g.

<sup>3</sup> The abbreviations used are: cKO, conditional knockout; qRT-PCR, quantitative real time PCR; SNP, single nucleotide polymorphism; ANOVA, analysis of variance.

genotype and arena in elevated plus maze). To determine the significance of drug treatment, a comparison of differences was used with an accompanying two-way ANOVA and a Bonferroni post hoc test as described (15). Statistical analysis was performed using Prism software (GraphPad, Inc.).

**Subjects for Human Genetics Analysis**—All participants are Caucasians and originate from a geographically isolated population living in Northern Sweden. In total, 351 patients diagnosed with bipolar disorder, 486 patients diagnosed with schizophrenia, and 512 healthy controls were included in this study. The mean ages at examination were 56.3 and 58.5 years and male percentages were 47.2 and 65.3% for bipolar disorder and schizophrenia patients, respectively. Experienced psychiatrists evaluated patients, and diagnosis was made according to DSM-IV criteria (48). Healthy controls were selected randomly from a longitudinal population-based study (the Betula project) and screened for history of psychotic events; their mean age at examination and the male/female ratio were similar to those of the patients. The control group was recruited from the same geographical region of northern Sweden as the patients, and there was no evidence of population stratification in these samples (using the Structure program for the analysis of several unlinked microsatellites). More information about these cohorts and the advantages of this isolated population for gene mapping can be found elsewhere (16). All subjects signed an informed consent and the project was approved by the institutional ethics committees of the Universities of Umea and Antwerp.

**Selection and Genotyping of Nicastrin SNPs**—To cover as much as possible genetic variation for *nicastrin*, the CEU genotype data were used from the *HapMap* database (17). Haplotype-tagging SNPs were chosen as predicted by Haploview (confidence interval minima for strong linkage disequilibrium; upper: 0.9 and lower: 0.65; upper confidence interval maximum for strong recombination: 0.9; fraction of strong linkage disequilibrium in informative comparisons must be at least: 0.9; exclude markers below 0.01 minor allele frequency). Only haplotypes with an estimated overall frequency of 5% or greater were considered in the selection analyses. Tagging SNPs not covered with the haplotype-tagging SNPs selection were added using the  $r^2$  option of *Tagger* (using a cutoff point of  $r^2 = 0.8$  and minor allele frequencies  $> 0.01$ ). SNPs located in regions with a high repeat content were excluded. The genomic locations of the 10 tagging SNPs analyzed in the *nicastrin* (NCSTN) gene are presented in Table 2. Genomic DNA was extracted from peripheral blood using standard methods. The genotyping of all SNPs was performed using the MassARRAY iPLEX Gold technology (Sequenom Inc., San Diego, CA), following the protocol provided by Sequenom. The PCR and extension primers were designed using Assay Design 3.0 (Sequenom Inc.). Analysis and scoring were performed using Typer 3.3 (Sequenom Inc.). All genotypes were manually checked by two independent researchers, and internal controls showed a good consistency of genotype results.

**Statistical Analysis of SNPs**—The PLINK and UNPHASED programs (18, 19) were used for Hardy-Weinberg equilibrium analysis, case-control comparisons of single SNPs (using a chi-squared test) and haplotypes in sliding windows (using 1.000

permutations). Block-wide haplotype determination and their case-control comparisons were carried out using the Haploview and UNPHASED programs (using 1.000 permutations) (20). Empirical  $p$  values for single SNPs were derived by permutation using PLINK and UNPHASED programs. Haplotype block structures and linkage disequilibrium patterns were visualized with Haploview.

## Results

**Construction of the Nicastrin cKO Mouse**—We conditionally deleted nicastrin, one of four core subunits of  $\gamma$ -secretase (21–23), from oligodendrocytes by crossing *olig1-cre* mice (11) (“Cre,” *olig1<sup>+/Cre</sup>*) with floxed *nicastrin* mice (10, 22) (“flox,” *nicastrin<sup>flox/flox</sup>*) to yield the *nicastrin* conditional knock-out mouse (“cKO,” *olig1<sup>+/Cre</sup>; nicastrin<sup>flox/flox</sup>*; Fig. 1a). cKO mice were viable, fertile, and born at Mendelian ratios. Deletion of the *nicastrin* gene from oligodendrocytes was confirmed by both recombination-specific PCR and qRT-PCR of the optic nerve, a heavily myelinated fiber tract rich in oligodendrocytes (Fig. 1, b and c). Recombination and restricted Cre expression to white matter tracts in the brain were also confirmed by using tdTomato reporter mice (data not shown). Direct visualization of nicastrin localization, however, was hampered by lack of antibodies suitable for immunostaining and will need to be addressed in the future. (Thus far, none of the commercial and noncommercial nicastrin antibodies we tested can specifically stain endogenous nicastrin when knock-out cells were used as controls.)

**Hypomyelination in the Nicastrin cKO Mouse**—Because of the nature of the conditional knock-out, *i.e.* selective deletion of nicastrin from oligodendrocytes, we asked whether conditional knock-out mice displayed altered myelination relative to control animals. Histological staining of whole brains with hematoxylin and eosin or Luxol fast blue/periodic acid Schiff did not reveal any gross pathology in neuroanatomy or myelination, particularly in white matter regions, such as the corpus callosum, striatum, and optic chiasm (data not shown). Ultrastructural inspection by electron microscopy, however, revealed thinner myelin sheaths in the optic nerve of cKO animals (Fig. 1d). Quantification of  $g$  ratios confirmed hypomyelination in the optic nerve, particularly of axons less than one micron in diameter (Fig. 1e; mean  $g$  ratio  $\pm$  S.D. for Cre =  $0.789 \pm 0.081$ , flox =  $0.778 \pm 0.100$ ; cKO =  $0.847 \pm 0.071$ ,  $p < 0.0001$ ). The effect on myelination was localized to the brain, because  $g$  ratio analysis in the spinal cord and sciatic nerve showed no difference between control and cKO mice (Fig. 1, f and g). These observations show that loss of nicastrin in oligodendrocytes leads to defective myelination in the brain.

**Behavioral Analysis of Nicastrin cKO Mice**—We next analyzed behavioral and functional outcomes of *nicastrin* deletion from the oligodendrocytes. We observed that *nicastrin* cKO mice were hyperactive and had increased exploratory behavior, as exhibited in positional activity recordings (Fig. 2a). (Here, “hyperactivity” is defined as increased movement without regard to the arena in which activity is measured, whereas “increased exploratory behavior” is defined as increased activity within a normally anxiogenic environment, *e.g.* the central arena in the open field maze). Hyperactivity was seen in both the open field (Fig. 2, b and c) and elevated plus maze (Fig. 2d).

## Schizophrenia- and OCD-like Behaviors in Nicastrin cKO Mice

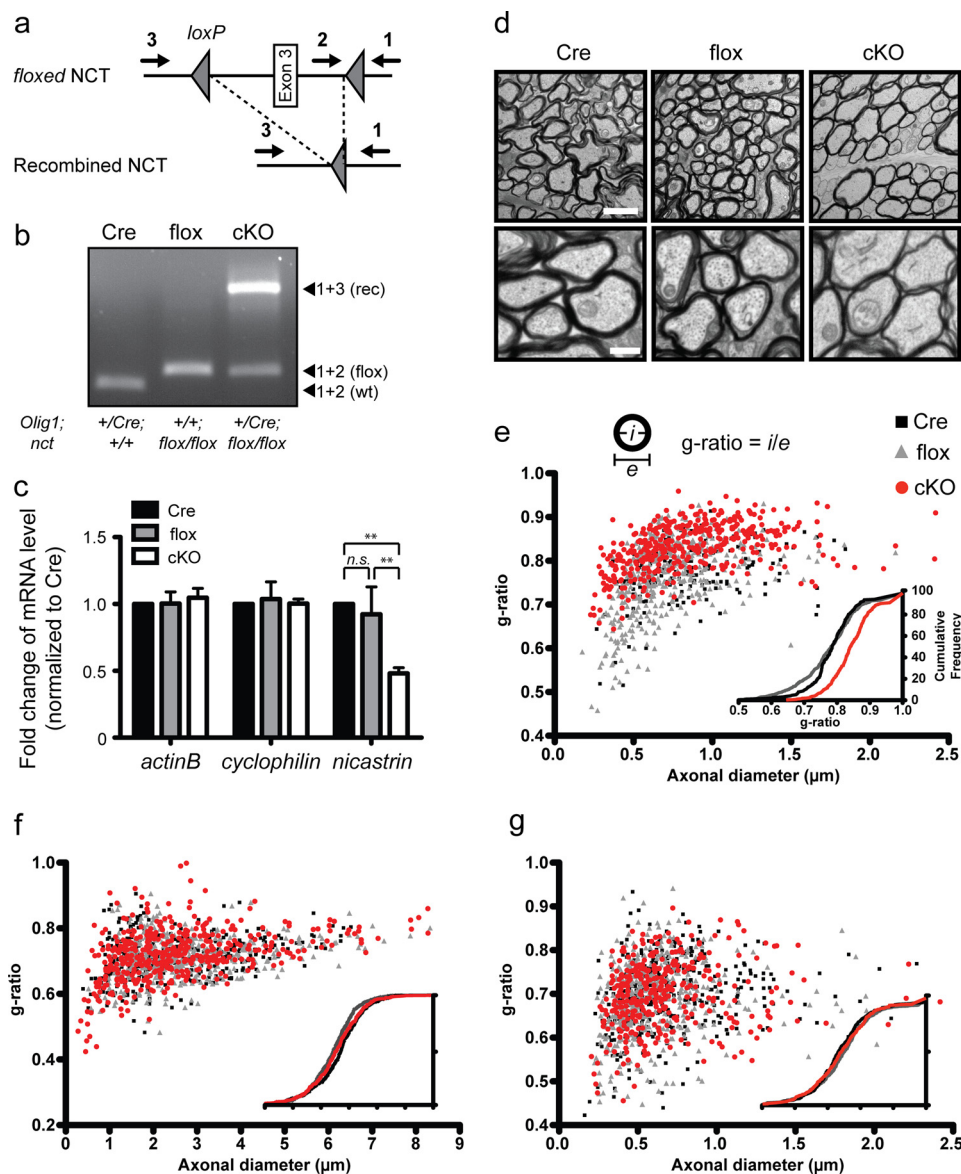


**FIGURE 1. *nicastrin* conditional knock-out mice have hypomyelination in the optic nerve but not in the spinal cord or periphery.** *a*, schematic for conditional deletion of nicastrin. Exon 3 of nicastrin is flanked by loxP sites. In the presence of Cre recombinase, exon 3 is excised, resulting in a truncated and nonfunctional nicastrin transcript. *b*, PCR of genomic DNA from optic nerves of the two control (Cre and flox) mice and the cKO mouse. Arrows represent genotyping primers. In the wild-type allele, primers 1 and 3 anneal at a distance too far for efficient amplification under standard PCR conditions (*a*). *c*, quantification of nicastrin transcripts from optic nerves of Cre, flox, and conditional knock-out mice. Also shown are two housekeeping genes as controls: *actinB* and *cyclophilin*. All data are normalized to a third housekeeping gene, *u36b*. The data represent the means  $\pm$  S.E. of three experimental replicates, with each experiment containing six pairs of optic nerves as sample material. *n.s.*,  $p > 0.05$ ; \*\*,  $p < 0.01$ . *d*, electron micrographs of the optic nerves from 5-month-old control or conditional knock-out mice. Scale bars, 2000 nm (upper row) and 500 nm (lower row). *e*, g-ratio plots for the optic nerves of control and conditional knock-out mice. *f*, g-ratio plots for the spinal cords of control and conditional knock-out mice. *g*, g-ratio plots for the sciatic nerve of control and conditional knock-out mice. The g-ratio is the ratio between the internal (i, i.e. axonal) and external (e, i.e. myelin) diameters (top); thus, an unmyelinated nerve has a g-ratio of 1.0. Insets, cumulative frequency plots with respect to g-ratio.

Likewise, conditional knock-out mice demonstrated increased exploratory behavior in both the open field and elevated plus mazes (Fig. 2, *e* and *f*). Hyperactivity and increased exploratory behavior are consistent with schizophrenia (24, 25). Indeed, cKO mice likewise displayed deficits in prepulse inhibition, a measure of sensorimotor gating, which is impaired in schizophrenia (Fig. 2*g*). Student's *t* tests with a minimum of four mice from each sex revealed no statistically significant difference in the performance of male and female mice on any of the measured behavioral tests (Table 1).

The neurotransmitter dopamine can modulate locomotor activity and plays an important role in schizophrenia (26). We therefore asked whether cKO mice were sensitive to haloperidol, a dopamine receptor antagonist used as a typical antipsychotic to treat schizophrenia. Acute intraperitoneal injection of a low dose of haloperidol reversed the hyperactivity of cKO animals to a level comparable with that of control animals (Fig. 3*a*). On the other hand, the low dose of haloperidol did not alter the thigmotaxis of control or cKO mice in an open field maze (Fig. 3*b*).

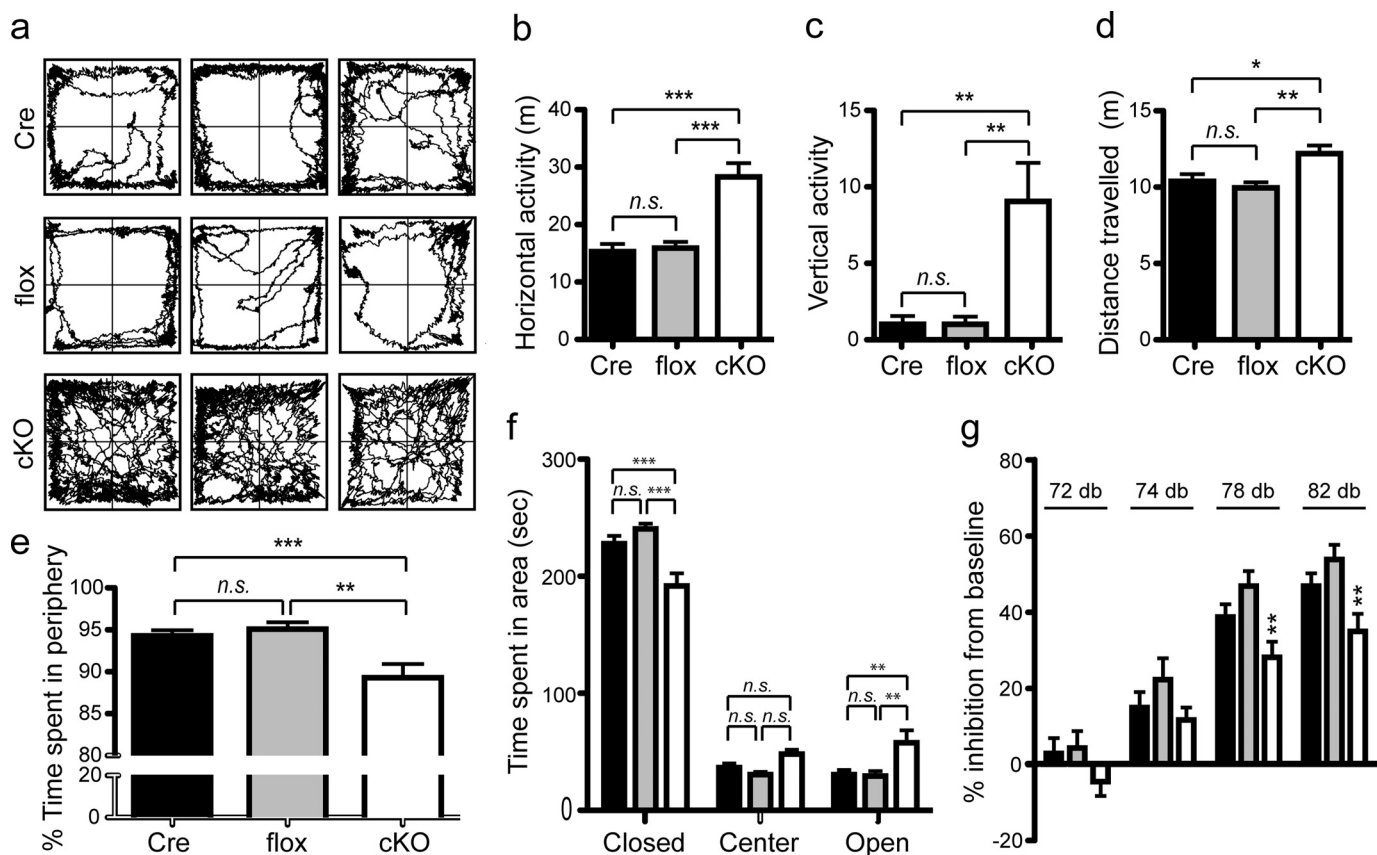


FIGURE 2. *Nicastrin* conditional knock-out mice display hyperlocomotion and increased exploratory behavior. *a*, representative activity recordings for four individual mice of each genotype as measured on force plate actimeters. *b*, distance traveled in the open field. *c*, vertical (rearing/jumping) activity. *d*, distance traveled in the elevated plus maze. *e*, open field test. *f*, elevated plus maze. *g*, inhibition to a prepulse tone ranging from 72 to 82 db. Models of schizophrenia are less sensitive to the prepulse and therefore show reduced inhibition. The data are presented as means  $\pm$  S.E. *n.s.*,  $p > 0.05$ ; \*,  $p < 0.05$ ; \*\*,  $p < 0.01$ ; \*\*\*,  $p < 0.001$ . A full table of descriptive statistics is provided in Table 1.

Aged *Nicastrin* cKO mice also exhibited extensive bald patches localized specifically to the nape of the neck and upper back; these bald patches progressed to full lesions with 100% penetrance by 9 months of age (Fig. 4, *a* and *b*). cKO mice displayed these lesions as early as 4 months of age, with a mean age of onset of  $28 \pm 5$  weeks (Fig. 4*b*). In most cases, the lesions were so severe as to warrant early termination under institutional animal care guidelines because of undue discomfort and distress. The lesions were self-inflicted and not caused by social grooming (allogrooming), because (i) singly housed cKO mice displayed the phenotype and (ii) when cohoused with control littermates, only cKO mice displayed this phenotype. Heterozygous *Nicastrin* conditional knock-out mice (*olig1*<sup>+/Cre</sup>; *Nicastrin*<sup>+/*flox*</sup>) did not present with lesions by 9 months of age (data not shown), suggesting that the lesion phenotype displayed by 9 months of age requires complete deletion of the *Nicastrin* gene. Given the link between *Nicastrin* and *acne inversa* (27), we examined skin pathology and itch response in cKO mice. Skin necropsy revealed local inflammation, but this appeared to be a secondary response to another primary insult. Indeed, lesions were not responsive to topical antibiotic, anti-inflammatory, or antihistamine treatment (data not shown). Suspecting an acute itch response, we tested the sensitivity to local injection of histamine but found no significant difference in response (data not shown).

Observation in home cages showed that cKO mice displayed compulsive grooming and trichotillomania (supplemental Video S1). Measurement of presymptomatic cKO mice revealed a trend toward excessive grooming both in terms of the number of grooming bouts and their duration (Fig. 4, *c* and *d*). The variability of grooming behavior among presymptomatic cKO mice (Fig. 4, *c* and *d*) may be compounded by hyperactivity. Moreover, it may reflect the variability in the age of onset of the lesion phenotype (Fig. 4*b*). Therefore, we observed these same mice throughout 10 months of age. Correlation analysis demonstrated that those mice that groomed most also were the first to display lesions, with strong negative correlations ( $p < 0.005$ ) between the extent of grooming and the age of lesion onset (Fig. 4, *e* and *f*).

**Identification of a SNP in *Nicastrin* in a Schizophrenia/Bipolar Disorder Cohort**—Because the *Nicastrin* gene resides near a schizophrenia susceptibility locus on chromosome 1 (28), we sought to identify *Nicastrin* SNPs in schizophrenia populations. We analyzed 10 tagging SNPs in the *Nicastrin* gene in 351 bipolar patients, 486 schizophrenia patients, and 512 healthy controls from Northern Sweden. All SNPs were in Hardy-Weinberg equilibrium, and the haplotype blocks compositions and minor allele frequencies were similar to those from the HapMap CEU samples (a “control” population). A significant association was found for SNP rs1802778 with the schizophrenia

# Schizophrenia- and OCD-like Behaviors in Nicastrin cKO Mice

**TABLE 1**  
Statistical analysis of mouse behavioral tests

Number of animals	Parameter	Comparison	Statistical test					
			F	p value				
<b>Open field</b>								
Cre	33	Horizontal activity (Fig. 2b)	Genotype	One-way ANOVA $F_{(2,73)} = 19.25$	<0.0001			
flox	25							
cKO	18							
Cre	35	Thigmotaxis (Fig. 2e)	Genotype	One-way ANOVA $F_{(2,76)} = 8.663$	0.0004			
flox	23							
cKO	21							
<b>Elevated plus maze</b>								
Cre	35	Horizontal activity (Fig. 2d)	Genotype	One-way ANOVA $F_{(2,78)} = 5.429$	0.0062			
flox	24							
cKO	22							
Cre	35	Time spent in area (Fig. 2f)	Genotype and arena	Two-way ANOVA $F_{(2,237)} = 0.07$	0.9284			
flox	24					Arena	$F_{(2,237)} = 877.16$	<0.0001
cKO	22					Interaction	$F_{(4,237)} = 13.10$	<0.0001
<b>Prepulse inhibition</b>								
Cre	33	Inhibition (Fig. 2g)	Genotype and intensity	Two-way ANOVA $F_{(2,414)} = 11.42$	<0.0001			
flox	28					Genotype	$F_{(3,414)} = 68.80$	<0.0001
cKO	47					Sound intensity	$F_{(6,414)} = 0.50$	0.8052
<b>Haloperidol (open field)</b>								
Cre	15	Horizontal activity (Fig. 3a)	Genotype and treatment	Two-way ANOVA on comparison of differences				
flox	8							
cKO	12					Differences between genotypes	$F_{(2,130)} = 6.25$	0.0026
		Treatment	$F_{(1,130)} = 7.25$	0.0080				
		Interaction	$F_{(2,130)} = 3.62$	0.0295				
		Genotype within treatment	One-way ANOVA					
		Vehicle	$F_{(2,63)} = 5.312$	0.0074				
		Haloperidol	$F_{(2,67)} = 1.540$	0.2218				
Cre	15	Thigmotaxis (Fig. 3b)	Genotype and treatment	Two-way ANOVA on comparison of differences				
flox	8							
cKO	12					Differences between genotypes	$F_{(2,126)} = 7.08$	0.0012
		Treatment	$F_{(1,126)} = 5.56$	0.0199				
		Interaction	$F_{(2,126)} = 0.43$	0.6501				
		Comparison of differences	One-way ANOVA					
		Vehicle	$F_{(2,63)} = 4.909$	0.0104				
		Haldol	$F_{(2,63)} = 3.672$	0.0310				
<b>Video recording</b>								
Cre	14	Vertical activity (Fig. 2c)	Genotype	One-way ANOVA $F_{(2,50)} = 6.585$	0.0029			
flox	16							
cKO	23							
Cre	14	Grooming bouts (Fig. 4c)	Genotype	One-way ANOVA $F_{(2,50)} = 3.729$	0.0309			
flox	16							
cKO	23							
cKO only	18	Grooming bouts vs. lesion age (Fig. 4e)	Genotype	Spearman correlation (nonparametric) $r_s[18] = -0.70$	0.0012			
Cre	14	Grooming duration (Fig. 4d)	Genotype	One-way ANOVA $F_{(2,50)} = 1.595$	0.2130			
flox	16							
cKO	23							
cKO only	18	Grooming duration vs. lesion age (Fig. 4f)	Genotype	Spearman correlation (nonparametric) $r_s[18] = -0.65$	0.0037			

sample ( $p = 0.039$ ; Table 2). We did not find significant associations with haplotypes using sliding windows or HapMap based haplotype blocks. The *nicastatin* SNP identified (rs1802778) resides in the 5' end of the gene and suggests a role in transcriptional or post-transcriptional regulation. Query of a publicly accessible database with genome-wide expression data (GTEx-Portal (29)) revealed significant changes in expression of *nicastatin* in both human whole blood ( $p = 1.1e-26$ ) and the caudate, a myelinated dopaminergic region of the striatum in the brain ( $p = 1.3E-06$ ). The SNP is also located in an exonic region of COPA (coatamer protein complex, subunit A), a protein involved in vesicular trafficking from the ER to the Golgi. Expression data from GTExPortal does not show any significant changes in COPA expression in the central

nervous system resulting from this SNP. Identification of nonsense or missense mutations in the genes for *nicastatin* and other  $\gamma$ -secretase subunits may provide further insight into the role of *nicastatin*/ $\gamma$ -secretase activity in myelination and psychiatric disease.

## Discussion

In this work, we present evidence that loss of *nicastatin* regulates myelination *in vivo* and that deficiency in the *nicastatin*  $\gamma$ -secretase subunit in oligodendrocytes results in hyperactivity and compulsive behaviors reminiscent of schizophrenia and obsessive-compulsive disorder. The mouse model from this study thus provides a new tool to explore the connections between myelination and psychiatric diseases and to dissect the

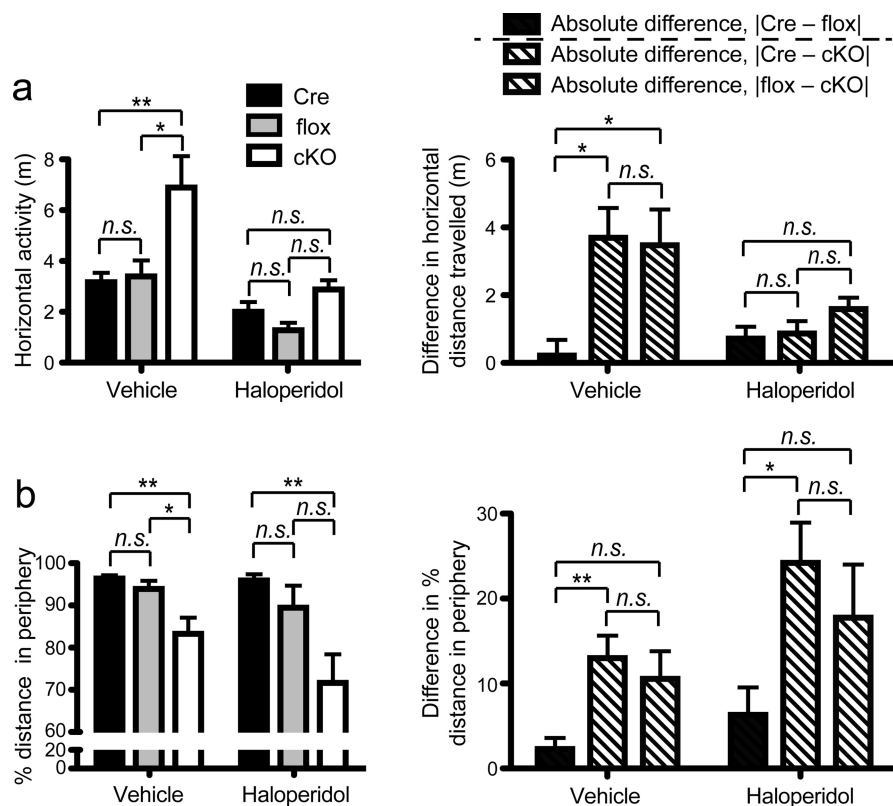


FIGURE 3. **Haloperidol restores the activity of nicastrin conditional knock-out mice.** Mice were administered low doses of haloperidol immediately prior to testing, and locomotion (*a*) and exploratory behavior (*b*) were measured in the open field as in Fig. 2. *Left panels*, statistical significance was determined by one-way ANOVA within a treatment group. The data are presented as means  $\pm$  S.E. *Right panels*, comparison of differences from *left panels* (15). The pairwise differences between each genotype and each treatment were then analyzed by two-way ANOVA as detailed under "Experimental Procedures." Shown is the statistical significance taken from Bonferroni post hoc tests. The data are presented as means  $\pm$  S.E. *n.s.*,  $p > 0.05$ ; \*,  $p < 0.05$ ; \*\*,  $p < 0.01$ . A full table of descriptive statistics is provided in Table 1.

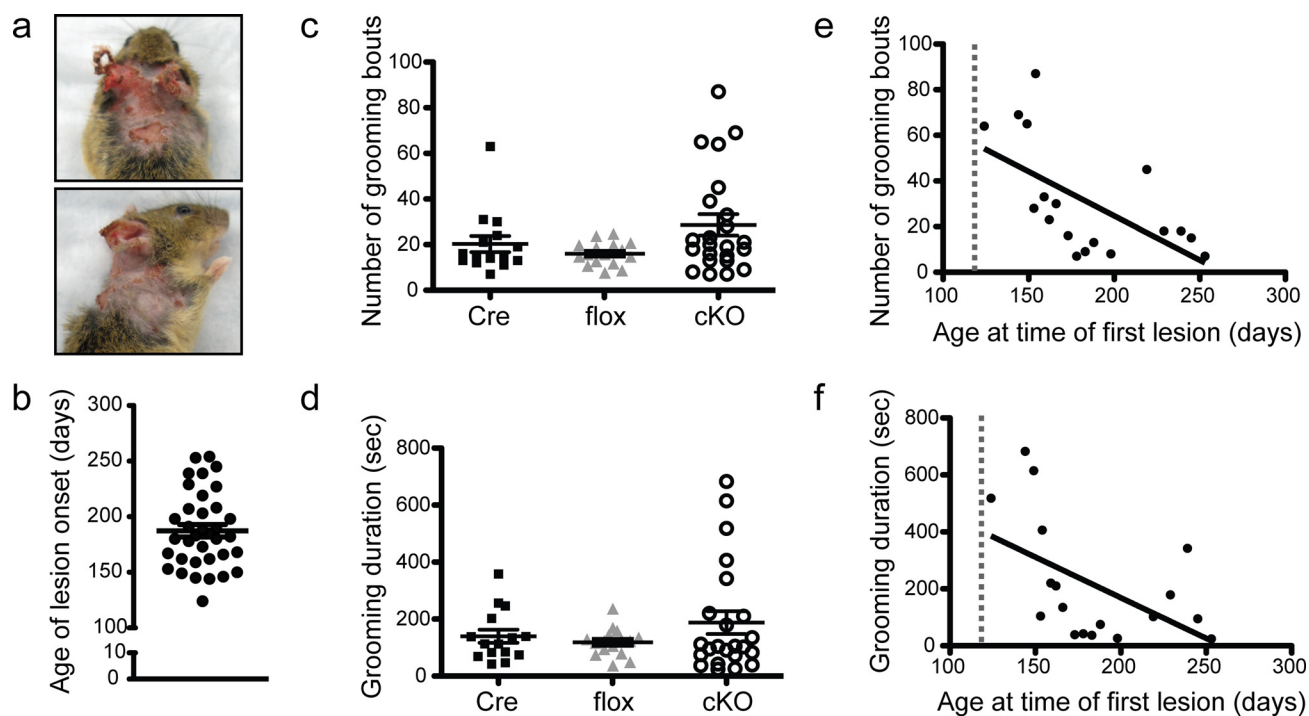


FIGURE 4. **nicastrin conditional knock-out mice display compulsive grooming.** *a*, representative image of a compulsively grooming female mouse 6 months of age. *b*, the age at which conditional knock-out mice develop lesions. *c–f*, number of grooming bouts (*c* and *e*) and duration of grooming (*d* and *f*) prior to the onset of lesions (gray vertical dotted line at 120 days, *e* and *f*). Spearman correlation analysis revealed strong negative correlations between both the age of lesion development and grooming bouts (*e*,  $r_s[18] = -0.70$ ,  $p = 0.0012$ ) and the age of lesion development and grooming duration (*f*,  $r_s[18] = -0.65$ ,  $p = 0.0037$ ). The data are presented as means  $\pm$  S.E. One-way ANOVA for *c*:  $F_{(2,50)} = 3.729$ ,  $p = 0.0309$ ; one-way ANOVA for *d*:  $F_{(2,50)} = 1.595$ ,  $p = 0.2130$ . A full table of descriptive statistics is provided in Table 1.

**TABLE 2**  
Selected HapMap SNPs in the *nicastrin* gene

Marker	dbSNP	Position	Distance	Region	Alleles	Genotype frequency BP/SZ/CO			Allele frequency BP/SZ/CO		HapMap MAF	<i>p</i> values	
						1/1	1/2	2/2	1	2		BP	SZ
						%			%				
SNP1	rs1802778	158570040	0	5'	C/T	29/23/30.8	49/51.8/45.7	22.1/25.3/23.5	53.4/48.9/53.7	46.6/51.1/46.3	0.42	0.711	0.039
SNP2	rs1324738	158579249	9209	5'	G/A	92.7/92.3/93.7	7/7.5/6.1	0.3/0.2/0.2	96.2/96/96.7	3.8/4/3.3	0.05	0.583	0.443
SNP3	rs6668576	1585685645	4396	Intron 2	C/T	31.2/25.8/32.6	49.7/51.7/45.5	19.1/22.5/21.9	56.1/51.7/55.3	43.9/48.3/44.7	0.44	0.994	0.100
SNP4	rs10494342	158583744	99	Intron 2	T/G	92.9/92.5/94.5	7.1/7.5/5.5	0/0/0	96.4/96.3/97.2	3.6/3.7/2.8	0.05	0.327	0.360
SNP5	rs2274184	158586213	2469	Intron 4	A/G	90.6/92.7/91.9	9.4/7.1/7.9	0/0.2/0.2	95.3/96.3/95.8	4.7/3.7/4.2	0.04	0.509	0.589
SNP6	rs6664438	158587983	1770	Intron 6	C/T	92.4/91.5/91.8	7/8.5/8.2	0.6/0/0	95.9/95.7/95.9	4.1/4.3/4.1	0.05	0.894	0.876
SNP7	rs6677637	158591395	3412	Intron 11	C/T	93.7/93/94.1	5.4/7/5.9	0.9/0/0	96.4/96.5/97.1	3.6/3.5/2.9	0.05	0.331	0.722
SNP8	rs6427515	158591735	340	Intron 11	C/T	89.5/88.6/90.5	9.6/11.4/9.3	0.9/0/0.2	94.3/94.3/95.1	5.7/5.7/4.9	0.08	0.354	0.606
SNP9	rs10797065	158598653	6918	3'	A/G	22.8/27.2/25.8	51.4/49.8/49	25.8/23/25.2	48.5/52.1/50.3	51.5/47.9/49.7	0.39	0.514	0.500
SNP10	rs17370655	158598705	52	3'	A/T	83.9/80.3/81.8	15.2/18.1/16.4	0.9/1.7/1.8	91.5/89.3/90	8.5/10.7/10	0.06	0.333	0.662

molecular mechanisms underlying behavioral abnormalities in the future. Of particular interest is the connection between  $\gamma$ -secretase and the Nrg1-ErbB4 pathway in schizophrenia. Nrg1 and ErbB4 have been linked to schizophrenia, and both proteins are substrates of  $\gamma$ -secretase (2, 3, 30, 31). Moreover, BACE1<sup>-/-</sup> mice (the upstream protease for Nrg1 cleavage) also show hyperactivity and prepulse inhibition deficits, as do our cKO mice (32). It has been reported that Nrg1-dependent ErbB4 cleavage by  $\gamma$ -secretase renders its intracellular domain to translocate to the nucleus to turn on myelin genes (33). Indeed, preliminary analysis of cKO mice by RNA-seq and quantitative PCR shows down-regulation of genes in the ErbB4 pathway, including myelin oligodendrocyte glycoprotein (mog) and myelin basic protein (mbp), as well as *erbb4* itself,<sup>4</sup> providing further support for the “myelination hypothesis” of schizophrenia.

The hyperactivity exhibited by our mice has also been shown in rodents that are partially deficient in the Aph1 subunit of  $\gamma$ -secretase (34, 35), although it is yet to be tested whether this is attributable to the loss of  $\gamma$ -secretase activity in oligodendrocytes. White matter abnormalities and changes in myelin genes have been linked to multiple psychiatric disorders (including schizophrenia and obsessive-compulsive behavior (9, 36)), as well as in Alzheimer disease (37). Meanwhile, recently identified models of compulsive grooming and trichotillomania similar to that displayed by our conditional knock-out mice involve genes important for neural (*i.e.* neuronal and glial) development, even though the phenotype does not present until adulthood (38–40). Given the role of  $\gamma$ -secretase in brain development, our conditional knock-out mice provide further evidence to support neural (including glial) development as a critical window in determining the later presentation of psychiatric disorders (41).

Psychiatric disorders are traditionally classified by clinical symptoms and behavioral abnormalities, which often overlap among different disorders. Hyperactivity or compulsive phenotypes are manifested in schizophrenia, obsessive-compulsive disease, attention deficit hyperactivity disorder, and autism. Interestingly, beyond impairment of memory and cognition, Alzheimer disease is also an attention disorder and as such shares behaviors reminiscent of attention deficit hyperactivity disorder and obsessive compulsive behavior (42). A subset of Alzheimer patients also exhibits psychosis (43, 44). The current

study advances a plausible hypothesis that aspects of these brain disorders are attributable to defective myelination and deficiency of  $\gamma$ -secretase, a pivotal developmental regulator for multiple developmental pathways.

On the other hand, the comorbidity of psychiatric illnesses has long been a challenge for classifying, studying, and treating these diseases. The high comorbidity of obsessive-compulsive and schizophrenic symptoms has puzzled clinicians and scientists over the past two centuries (45–47). Although schizophrenia and obsessive-compulsive disorder are now considered separate entities, it is still unclear whether these conditions co-occur simply by chance or they share a fundamental biological basis. Our work now provides a conceptual and mechanistic framework, as well as a unique animal model, for the shared biology of these comorbid conditions, strongly supporting the view that schizophrenia with obsessive-compulsive disorder is a distinct subtype of schizophrenia.

**Author Contributions**—D. R. D., Y. Z., Y.-H. H., Q. R. L., S. G. B., and G. Y. designed mouse experiments. D. R. D., Y. Z., B. C., J. A., Y.-H. H., C. Y., and S. G. B. performed mouse experiments. D. R. D., Y. Z., M. A., and S. G. B. analyzed mouse behavioral data. D. R. D., Y. Z., M. M. B., and J. M. W. maintained the mouse colony and performed genotyping analysis. A. N. and R. A. collected and phenotyped the Swedish samples for genetic analysis. D. A. F. performed the genotyping and statistical analysis for the human genetics study. J.D.-F. designed the genotyping study. P. C. identified nicastrin as a candidate gene for analysis in schizophrenia. Q. R. L. provided *olig1<sup>+/-Cre</sup>* mice and offered technical advice on myelination experiments. D. R. D., J. D.-F., P. C., and G. Y. prepared the manuscript.

**Acknowledgments**—We thank T. Südhof for the generous gift of the floxed *nicastrin* mice. We thank B. de Strooper, Z. Vegh, R. Gereaux, and C. Sephton for thoughtful discussion of this work. We acknowledge the technical contribution of the personnel of the University of Texas Southwestern Rodent Behavior Core and the VIB Genetic Service Facility, and we thank K. Kysor and A. Chamberlain for technical assistance.

## References

- Dries, D. R., and Yu, G. (2008) Assembly, maturation, and trafficking of the  $\gamma$ -secretase complex in Alzheimer's disease. *Curr. Alzheimer Res.* 5, 132–146
- Stefansson, H., Sigurdsson, E., Steinthorsdottir, V., Bjornsdottir, S., Sigmundsson, T., Ghosh, S., Brynjolfsson, J., Gunnarsdottir, S., Ivarsson, O., Chou, T. T., Hjaltason, O., Birgisdottir, B., Jonsson, H., Gudnadottir, V. G., Gudmundsdottir, E., *et al.* (2002) Neuregulin 1 and susceptibility to schiz-

<sup>4</sup>Y. Zhu, A. Kulkarni, D. R. Dries, and G. Yu, manuscript in preparation.



- ophrenia. *Am. J. Hum. Genet.* **71**, 877–892
3. Jaaro-Peled, H., Hayashi-Takagi, A., Seshadri, S., Kamiya, A., Brandon, N. J., and Sawa, A. (2009) Neurodevelopmental mechanisms of schizophrenia: understanding disturbed postnatal brain maturation through neuregulin-1-ErbB4 and DISC1. *Trends Neurosci.* **32**, 485–495
  4. Young-Pearse, T. L., Suth, S., Luth, E. S., Sawa, A., and Selkoe, D. J. (2010) Biochemical and functional interaction of disrupted-in-schizophrenia 1 and amyloid precursor protein regulates neuronal migration during mammalian cortical development. *J. Neurosci.* **30**, 10431–10440
  5. Hu, Q. D., Ang, B. T., Karsak, M., Hu, W. P., Cui, X. Y., Duka, T., Takeda, Y., Chia, W., Sankar, N., Ng, Y. K., Ling, E. A., Maciag, T., Small, D., Trifonova, R., Kopan, R., *et al.* (2003) F3/contactin acts as a functional ligand for Notch during oligodendrocyte maturation. *Cell* **115**, 163–175
  6. Blobel, C. P., Carpenter, G., and Freeman, M. (2009) The role of protease activity in ErbB biology. *Exp. Cell Res.* **315**, 671–682
  7. Mi, S., Lee, X., Hu, Y., Ji, B., Shao, Z., Yang, W., Huang, G., Walus, L., Rhodes, K., Gong, B. J., Miller, R. H., and Pepinsky, R. B. (2011) Death receptor 6 negatively regulates oligodendrocyte survival, maturation and myelination. *Nat. Med.* **17**, 816–821
  8. Roy, K., Murtie, J. C., El-Khodori, B. F., Edgar, N., Sardi, S. P., Hooks, B. M., Benoit-Marand, M., Chen, C., Moore, H., O'Donnell, P., Brunner, D., and Corfas, G. (2007) Loss of erbB signaling in oligodendrocytes alters myelin and dopaminergic function, a potential mechanism for neuropsychiatric disorders. *Proc. Natl. Acad. Sci. U.S.A.* **104**, 8131–8136
  9. Takahashi, N., Sakurai, T., Davis, K. L., and Buxbaum, J. D. (2011) Linking oligodendrocyte and myelin dysfunction to neurocircuitry abnormalities in schizophrenia. *Prog. Neurobiol.* **93**, 13–24
  10. Tabuchi, K., Chen, G., Südhof, T. C., and Shen, J. (2009) Conditional forebrain inactivation of nicastrin causes progressive memory impairment and age-related neurodegeneration. *J. Neurosci.* **29**, 7290–7301
  11. Xin, M., Yue, T., Ma, Z., Wu, F. F., Gow, A., and Lu, Q. R. (2005) Myelination and axonal recognition by oligodendrocytes in brain are uncoupled in Olig1-null mice. *J. Neurosci.* **25**, 1354–1365
  12. Autry, A. E., Adachi, M., Nosyreva, E., Na, E. S., Los, M. F., Cheng, P. F., Kavalali, E. T., and Monteggia, L. M. (2011) NMDA receptor blockade at rest triggers rapid behavioural antidepressant responses. *Nature* **475**, 91–95
  13. Blundell, J., Blais, C. A., Etherton, M. R., Espinosa, F., Tabuchi, K., Walz, C., Bolliger, M. F., Südhof, T. C., and Powell, C. M. (2010) Neuroigin-1 deletion results in impaired spatial memory and increased repetitive behavior. *J. Neurosci.* **30**, 2115–2129
  14. Simón, V. M., Parra, A., Miarro, J., Arenas, M. C., Vinader-Caerols, C., and Aguilár, M. A. (2000) Predicting how equipotent doses of chlorpromazine, haloperidol, sulpiride, raclopride and clozapine reduce locomotor activity in mice. *Eur. Neuropsychopharmacol.* **10**, 159–164
  15. Nieuwenhuis, S., Forstmann, B. U., and Wagenmakers, E. J. (2011) Erroneous analyses of interactions in neuroscience: a problem of significance. *Nat. Neurosci.* **14**, 1105–1107
  16. Venken, T., and Del-Favero, J. (2007) Chasing genes for mood disorders and schizophrenia in genetically isolated populations. *Hum. Mutat.* **28**, 1156–1170
  17. Altshuler, D. M., Gibbs, R. A., Peltonen, L., Altshuler, D. M., Gibbs, R. A., Peltonen, L., Dermitzakis, E., Schaffner, S. F., Yu, F., Peltonen, L., Dermitzakis, E., Bonnen, P. E., Altshuler, D. M., Gibbs, R. A., de Bakker, P. I., *et al.* (2010) Integrating common and rare genetic variation in diverse human populations. *Nature* **467**, 52–58
  18. Dudbridge, F. (2008) Likelihood-based association analysis for nuclear families and unrelated subjects with missing genotype data. *Hum. Hered.* **66**, 87–98
  19. Purcell, S., Neale, B., Todd-Brown, K., Thomas, L., Ferreira, M. A., Bender, D., Maller, J., Sklar, P., de Bakker, P. I., Daly, M. J., and Sham, P. C. (2007) PLINK: a tool set for whole-genome association and population-based linkage analyses. *Am. J. Hum. Genet.* **81**, 559–575
  20. Barrett, J. C., Fry, B., Maller, J., and Daly, M. J. (2005) Haploview: analysis and visualization of LD and haplotype maps. *Bioinformatics* **21**, 263–265
  21. Dries, D. R., Shah, S., Han, Y. H., Yu, C., Yu, S., Shearman, M. S., and Yu, G. (2009) Glu-333 of nicastrin directly participates in  $\gamma$ -secretase activity. *J. Biol. Chem.* **284**, 29714–29724
  22. Shah, S., Lee, S. F., Tabuchi, K., Hao, Y. H., Yu, C., LaPlant, Q., Ball, H., Dann, C. E., 3rd, Südhof, T., and Yu, G. (2005) Nicastrin functions as a  $\gamma$ -secretase-substrate receptor. *Cell* **122**, 435–447
  23. Yu, G., Nishimura, M., Arawaka, S., Levitan, D., Zhang, L., Tandon, A., Song, Y. Q., Rogava, E., Chen, F., Kawarai, T., Supala, A., Levesque, L., Yu, H., Yang, D. S., Holmes, E., *et al.* (2000) Nicastrin modulates presenilin-mediated notch/glp-1 signal transduction and  $\beta$ APP processing. *Nature* **407**, 48–54
  24. Hikida, T., Jaaro-Peled, H., Seshadri, S., Oishi, K., Hookway, C., Kong, S., Wu, D., Xue, R., Andradé, M., Tankou, S., Mori, S., Gallagher, M., Ishizuka, K., Pletnikov, M., Kida, S., and Sawa, A. (2007) Dominant-negative DISC1 transgenic mice display schizophrenia-associated phenotypes detected by measures translatable to humans. *Proc. Natl. Acad. Sci. U.S.A.* **104**, 14501–14506
  25. Kuroda, K., Yamada, S., Tanaka, M., Iizuka, M., Yano, H., Mori, D., Tsuboi, D., Nishioka, T., Namba, T., Iizuka, Y., Kubota, S., Nagai, T., Ibi, D., Wang, R., Enomoto, A., *et al.* (2011) Behavioral alterations associated with targeted disruption of exons 2 and 3 of the Disc1 gene in the mouse. *Hum. Mol. Genet.* **20**, 4666–4683
  26. Howes, O. D., and Kapur, S. (2009) The dopamine hypothesis of schizophrenia: version III—the final common pathway. *Schizophr. Bull.* **35**, 549–562
  27. Wang, B., Yang, W., Wen, W., Sun, J., Su, B., Liu, B., Ma, D., Lv, D., Wen, Y., Qu, T., Chen, M., Sun, M., Shen, Y., and Zhang, X. (2010)  $\gamma$ -Secretase gene mutations in familial acne inversa. *Science* **330**, 1065
  28. Allen, N. C., Bagade, S., McQueen, M. B., Ioannidis, J. P., Kavvoura, F. K., Khoury, M. J., Tanzi, R. E., and Bertram, L. (2008) Systematic meta-analyses and field synopsis of genetic association studies in schizophrenia: the SzGene database. *Nat. Genet.* **40**, 827–834
  29. GTEx Consortium (2015) Human genomics. The Genotype-Tissue Expression (GTEx) pilot analysis: multitissue gene regulation in humans. *Science* **348**, 648–660
  30. Ni, C. Y., Murphy, M. P., Golde, T. E., and Carpenter, G. (2001)  $\gamma$ -Secretase cleavage and nuclear localization of ErbB-4 receptor tyrosine kinase. *Science* **294**, 2179–2181
  31. De Strooper, B., Iwatsubo, T., and Wolfe, M. S. (2012) Presenilins and  $\gamma$ -secretase: structure, function, and role in Alzheimer disease. *Cold Spring Harb. Perspect. Med.* **2**, a006304
  32. Savonenko, A. V., Melnikova, T., Laird, F. M., Stewart, K. A., Price, D. L., and Wong, P. C. (2008) Alteration of BACE1-dependent NRG1/ErbB4 signaling and schizophrenia-like phenotypes in BACE1-null mice. *Proc. Natl. Acad. Sci. U.S.A.* **105**, 5585–5590
  33. Lai, C., and Feng, L. (2004) Implication of  $\gamma$ -secretase in neuregulin-induced maturation of oligodendrocytes. *Biochem. Biophys. Res. Commun.* **314**, 535–542
  34. Dejaegere, T., Serneels, L., Schäfer, M. K., Van Biervliet, J., Horr , K., Depboylu, C., Alvarez-Fischer, D., Herreman, A., Willem, M., Haass, C., Höglinger, G. U., D'Hooge, R., and De Strooper, B. (2008) Deficiency of Aph1B/C- $\gamma$ -secretase disturbs Nrg1 cleavage and sensorimotor gating that can be reversed with antipsychotic treatment. *Proc. Natl. Acad. Sci. U.S.A.* **105**, 9775–9780
  35. Coolen, M. W., Van Loo, K. M., Van Bakel, N. N., Pulford, D. J., Serneels, L., De Strooper, B., Ellenbroek, B. A., Cools, A. R., and Martens, G. J. (2005) Gene dosage effect on  $\gamma$ -secretase component Aph-1b in a rat model for neurodevelopmental disorders. *Neuron* **45**, 497–503
  36. Fields, R. D. (2008) White matter in learning, cognition and psychiatric disorders. *Trends Neurosci.* **31**, 361–370
  37. Meier, I. B., Manly, J. J., Provenzano, F. A., Louie, K. S., Wasserman, B. T., Griffith, E. Y., Hector, J. T., Allocco, E., and Brickman, A. M. (2012) White matter predictors of cognitive functioning in older adults. *J. Int. Neuropsychol. Soc.* **18**, 414–427
  38. Greer, J. M., and Capocchi, M. R. (2002) Hoxb8 is required for normal grooming behavior in mice. *Neuron* **33**, 23–34
  39. Shmelkov, S. V., Hormigo, A., Jing, D., Proenca, C. C., Bath, K. G., Milde, T., Shmelkov, E., Kushner, J. S., Baljevic, M., Dincheva, I., Murphy, A. J., Valenzuela, D. M., Gale, N. W., Yancopoulos, G. D., Ninan, I., Lee, F. S., and Rafii, S. (2010) Slitrk5 deficiency impairs corticostriatal circuitry and leads to obsessive-compulsive-like behaviors in mice.

## Schizophrenia- and OCD-like Behaviors in Nicastrin cKO Mice

- Nat. Med.* **16**, 598–602
40. Welch, J. M., Lu, J., Rodriguiz, R. M., Trotta, N. C., Peca, J., Ding, J. D., Feliciano, C., Chen, M., Adams, J. P., Luo, J., Dudek, S. M., Weinberg, R. J., Calakos, N., Wetsel, W. C., and Feng, G. (2007) Cortico-striatal synaptic defects and OCD-like behaviours in Sapap3-mutant mice. *Nature* **448**, 894–900
  41. Casey, B. J., Pattwell, S. S., Glatt, C. E., and Lee, F. S. (2013) Treating the developing brain: implications from human imaging and mouse genetics. *Annu. Rev. Med.* **64**, 427–439
  42. Romberg, C., Bussey, T. J., and Saksida, L. M. (2013) Paying more attention to attention: towards more comprehensive cognitive translation using mouse models of Alzheimer's disease. *Brain Res. Bull.* **92**, 49–55
  43. Murray, P. S., Kirkwood, C. M., Gray, M. C., Ikonovic, M. D., Paljug, W. R., Abrahamson, E. E., Henteloff, R. A., Hamilton, R. L., Kofler, J. K., Klunk, W. E., Lopez, O. L., Penzes, P., and Sweet, R. A. (2012)  $\beta$ -Amyloid 42/40 ratio and kalirin expression in Alzheimer disease with psychosis. *Neurobiol. Aging* **33**, 2807–2816
  44. Spalletta, G., Girardi, P., Caltagirone, C., and Orfei, M. D. (2012) Anosognosia and neuropsychiatric symptoms and disorders in mild Alzheimer disease and mild cognitive impairment. *J. Alzheimers Dis.* **29**, 761–772
  45. Berrios, G. E. (1989) Obsessive-compulsive disorder: its conceptual history in France during the 19th century. *Compr. Psychiatry* **30**, 283–295
  46. Bottas, A., Cooke, R. G., and Richter, M. A. (2005) Comorbidity and pathophysiology of obsessive-compulsive disorder in schizophrenia: is there evidence for a schizo-obsessive subtype of schizophrenia? *J. Psychiatry Neurosci.* **30**, 187–193
  47. Buckley, P. F., Miller, B. J., Lehrer, D. S., and Castle, D. J. (2009) Psychiatric comorbidities and schizophrenia. *Schizophr. Bull.* **35**, 383–402
  48. American Psychological Association (1994) *Diagnostic and Statistical Manual of Mental Disorders*, 4th Ed, American Psychological Association, Washington, D. C.